

Motion of a ball dropped onto a one-dimensional self-affine surface

This article has been downloaded from IOPscience. Please scroll down to see the full text article.

1997 J. Phys. A: Math. Gen. 30 4915

(<http://iopscience.iop.org/0305-4470/30/14/007>)

View [the table of contents for this issue](#), or go to the [journal homepage](#) for more

Download details:

IP Address: 171.66.16.108

The article was downloaded on 02/06/2010 at 05:48

Please note that [terms and conditions apply](#).

Motion of a ball dropped onto a one-dimensional self-affine surface

Harold Auradou[†], Daniel Bideau[†], Alex Hansen[‡] and Knut Jørgen Måløy[§]

[†] Groupe Matière Condensée et Matériaux, URA CNRS 807, Université de Rennes 1, F-35042 Rennes Cedex, France

[‡] Institutt for fysikk, Norges teknisk-naturvitenskapelige universitet, N-7034 Trondheim, Norway

[§] Fysisk institutt, Universitetet i Oslo, Postboks 1048 Blindern, N-0316 Oslo, Norway

Received 24 July 1996, in final form 15 January 1997

Abstract. We present a molecular dynamics study of the subsequent dissipation-free motion of a ball dropped onto a self-affine profile characterized by the Hurst exponent H . The distribution of sizes of the energetically accessible intervals to which the ball is confined as a function of the height h at which the ball is dropped has been determined. Furthermore, the correlations between the distribution of slopes of the profiles and the distribution of directions of the velocity vector at impact were studied. We found that the distribution of angles the velocity vector makes with the normal of the profile is independent of both H and the roughness amplitude. The distribution of horizontal lengths of the parabolic trajectories of the ball between impacts were further studied, and we found it to be a power law with exponent $H - 2$ for small lengths and Gaussian-like for large lengths. Finally, we discuss the scaling of the parameters of the particle trajectory with respect to rescaling of the self-affine surface on which the ball bounces.

It is only recently that the physics community has taken on the challenge posed by the dynamics of granular materials, despite its obvious technological importance. One reason for this may be found in the great difficulties of gaining a theoretical understanding of the phenomena involved when only analytical tools were at hand. The situation is, however, rapidly changing as computers become more and more powerful. As a result, one is not only seeing a rapidly advancing theoretical understanding of the phenomena involved, but new phenomena are discovered at a high rate, see e.g. [1–3].

Through this surge of interest in this field, it has become clear that even the seemingly simple problem of the dynamics of one single grain interacting with a set of boundaries is far from completely understood. For example, it came as a surprise that the effective force felt by a ball rolling on an inclined bumpy surface is proportional to the velocity of the ball [4]. A theoretical explanation of this effect has only recently been suggested [5]. Since the mid 1980s, it has been recognized that the motion of a single grain dropped onto a flat but oscillating surface may give rise to very complex chaotic behaviour, see e.g. [6–16].

In this paper, we study the problem of a single grain dropped onto a static but rough surface. This is the ‘quenched disorder’ version of the bouncing ball on a vibrating surface problem, in the sense that the impact point between the ball and the surface depends here only on the horizontal coordinate of the ball and not on time. More generally, the energy exchange between a rough wall and an ensemble of particles is a central problem in granular

flow and this study may be regarded as being one step in the direction of understanding this complex problem.

Naturally occurring rough surfaces normally have long-range correlations built into them. These correlations typically manifest themselves through the surfaces being *self-affine*, meaning that they are statistically invariant under the transformation $x \rightarrow \lambda x$ and $y \rightarrow \lambda^H y$. Here H is the *Hurst exponent*, and where $0 < H < 1$ [21]. This invariance leads to, for example the correlation function $\pi(\delta h, \delta x)$, giving the probability density to find a height difference δh over a horizontal distance δx , scaling as

$$\lambda^H \pi(\lambda^H \delta h, \lambda \delta x) = \pi(\delta h, \delta x). \quad (1)$$

The prefactor λ^H is found by the normalization of $\pi(\delta h, \delta x)$.

The surfaces that we consider in this paper are self-affine. Our emphasis is on the geometrical constraints of the motion of the ball rather than on its detailed dynamics such as is the case in the analysis of the chaotic motion of a jumping ball on a vibrating surface. We note how problems with quenched disorder are notoriously much more difficult to treat theoretically than those with annealed disorder.

We consider a one-dimensional self-affine profile consisting of facets of size l when projected onto the horizontal plane. The facets have a length l measured along the horizontal. Furthermore, the height difference between consecutive corners of the profile is Gaussian of width ϵ and zero mean. The radius of the ball is r , and we assume $r \ll l$. The gravitational field g points downwards, i.e. in the negative u direction. There is no inclination of the self-affine surface. This means that we orient it in such a way that its two endpoints are at the same vertical height. Our numerical studies are based on molecular dynamics simulations using an event-driven algorithm.

In the following, we construct the probability $d\Delta N(\Delta, h)$ that a horizontal interval of size Δ is energetically accessible to a ball dropped from a height h above the self-affine surface $y(x)$ at $x = x_0$. We define Δ more precisely: If, for a given profile, x_- is the largest x smaller than x_0 such that $y(x_-) = y(x_0) + h$, and x_+ is the smallest x larger than x_0 such that $y(x_+) = y(x_0) + h$, then $\Delta = x_+ - x_-$, see figure 1.

We assume that $N(\Delta, h)$ has the structure

$$N(\Delta, h) = \frac{h^\beta}{\Delta^\alpha} G\left(\frac{h}{\Delta^\gamma}\right) \quad (2)$$

where the function $G(z)$ tends towards a constant for small values of z and falls off faster than any power law for large z . When $h \rightarrow 0$, N is simply the first return probability of the profile $y(x)$. It was shown in Hansen *et al* [18] that the first return probability density

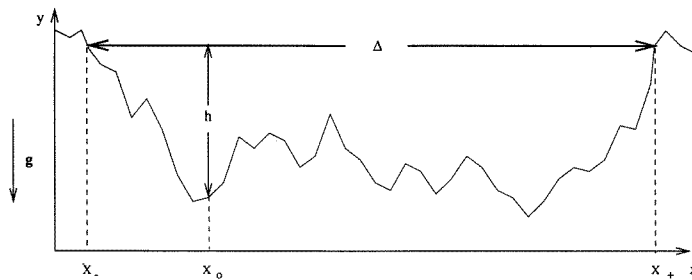


Figure 1. This figure defines Δ and other relevant quantities.

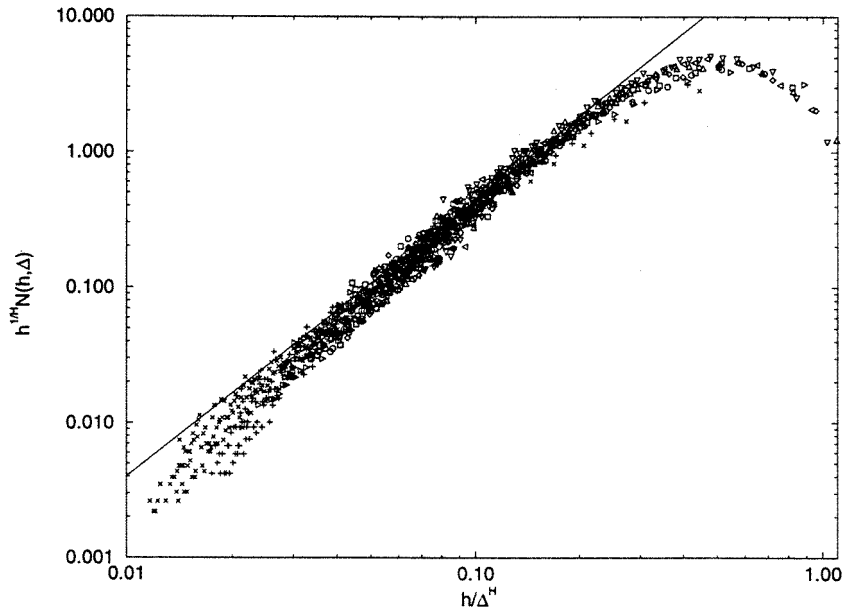


Figure 2. $h^{1/H}N(\Delta, h)$ plotted against h/Δ^H for different h . The slope of the straight line is $2/H - 1$.

$N_f(\Delta) \sim \Delta^{-(2-H)}$. Thus,

$$\alpha = 2 - H. \quad (3)$$

Self affinity demands that $d\Delta N(\Delta, h)$ is invariant under the rescaling $x \rightarrow \lambda x$ and $h \rightarrow \lambda^H h$, i.e.

$$d\Delta N(\Delta, h) = d(\lambda\Delta)N(\lambda\Delta, \lambda^H h). \quad (4)$$

Combining this equation with (2) and (3), we find

$$\beta = \frac{1 - H}{H} \quad (5)$$

and

$$\gamma = H. \quad (6)$$

Setting $H = \frac{1}{2}$, so that the profile $y = y(x)$ corresponds to a random walk, $N(\Delta, h)$ is readily found to be [19]

$$N(\Delta, h) = \frac{he^{-h^2/2\Delta}}{(4\pi\Delta)^{3/2}} \quad (7)$$

which is consistent with (2), with the exponents given in (3), (5) and (6).

In order to test (2) numerically, we measured $N(\Delta, h)$ from 1000 samples of length $L = 10^4$ facets and $H = 0.7$ † using the Mandelbrot–Van Ness algorithm to generate the profiles [20, 21]. In figure 2 we show $h^{1/H}N(\Delta/h)$ as a function of h/Δ^H . The slope of the straight line is $2/H - 1 = 1.86$ which is consistent with (2).

† We have chosen to study $H = 0.7$ since it is this value that is found for two-dimensional fractures, see [24–27].

The average size of Δ in a system of size L is

$$\langle \Delta \rangle = \int^L \Delta N(\Delta, h) d\Delta = CL^H h^\beta \quad (8)$$

in the limit of large L . Thus, the average diverges as $L \rightarrow \infty$. We have thus the interesting situation that a ball dropped from any height above an infinitely long self-affine profile will be trapped in a finite-sized interval, since $N(\Delta, h) \rightarrow 0$ for $L \rightarrow \infty$ without discontinuities. It will be *localized*. However, the average size of the interval in which the ball is trapped is infinite. This illustrates well the point made by Anderson [22] in connection with localization of electrons: If one searches for localization after averaging over samples, none are found. However, reversing the order leads to localization. In our case, the ball is always trapped. However, when posing the question whether the ball is trapped or not after averaging over samples, one will be led to the opposite conclusion.

The distribution of the tangent of the angle α between the facets of our surfaces and the horizontal, $a = \tan(\alpha)$, is

$$g(a) = \frac{e^{-a^2/2\epsilon^2}}{\sqrt{2\pi\epsilon^2}}. \quad (9)$$

Using an event-driven molecular dynamics algorithm, we drop the ball from a height h above the profile at $x = x_0$. The initial velocity of the ball is zero. Let v_x and v_y be the horizontal and vertical components of the velocity. At the point of impact between the ball and the profile at x , we have

$$(v_x^2 + v_y^2) = 2g(h - y(x)). \quad (10)$$

We note that this is the equation of a circle with a radius given by the height $y(x)$. The largest radius corresponds to the minimum of the profile reachable by the ball, and the minimal radius, which is zero, corresponds to x_- and x_+ . In figure 3 we plot v_y against v_x for a sequence of impacts on a given profile. We note that some levels are ‘visited’ more often than others. In fact, those radii correspond to local minima, which tend to capture the ball.

We define $\beta = \arctan(v_x/v_y)$ at impact, see figure 4. It is interesting to study the distribution $p(\beta)$ for profiles generated with different ϵ , which is defined in equation (9). A larger ϵ corresponds to a more pointed profile, i.e. its amplitude is larger. In figure 5 we show $p(\beta)$ for different ϵ . We note in this figure how the maximum of the distribution splits into two for larger ϵ . This is caused by the ball having an increasing tendency to jump between opposite slopes of deep valleys.

We now ask the question: What is the distribution of the angles of the facets that is hit by the ball, compared with the distribution of all the facets, (9)? In figure 6 we show the distribution of $\tan(\alpha)$ of the facets that were hit by the ball. Clearly, it is very far from a Gaussian. Moreover, it changes character quite dramatically with different values of the parameters ϵ and H . In particular, we note that for the smaller $\epsilon = 0.274$ and $H = 0.5$, the distribution of tangents has a single maximum at the origin, while for the same ϵ but $H = 0.7$, the single maximum is split into two. This is a reflection of the persistence of self-affine surfaces with $H > 0.5$: they have a tendency to move in the direction they were already heading. This creates ‘valleys’ in which the ball jump from one slope to the opposite one. On the other hand, for $\epsilon = 1.6$, there seems to be little effect of the change of Hurst exponent. The reason for this is that the large value of ϵ produces a similar ‘valley’ effect, but on a scale which is so small that difference in large-scale features of the profiles implied by the different Hurst exponents is not visible.

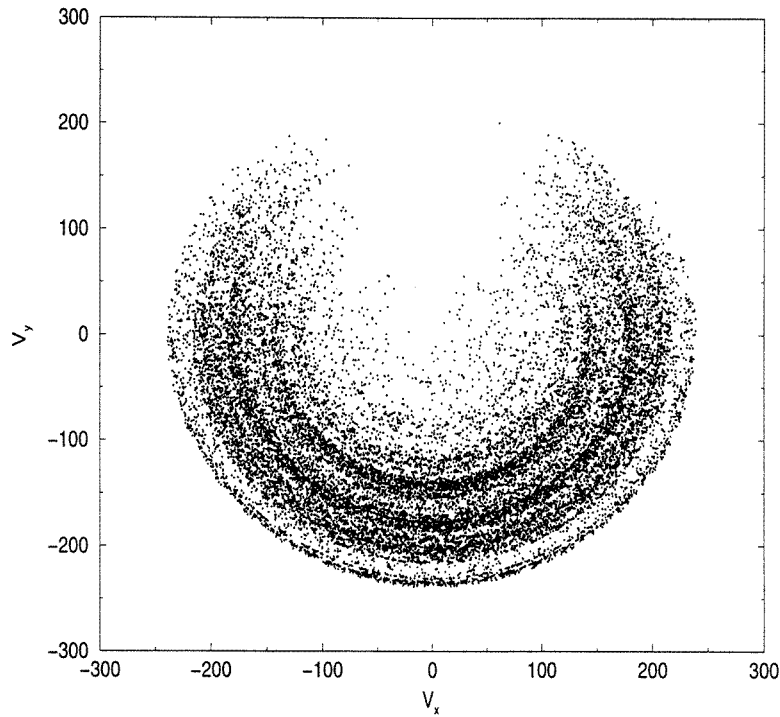


Figure 3. v_y as a function of v_x at each of the 5000 contacts for a given profile with $H = 0.7$ and $\epsilon = 0.5$.

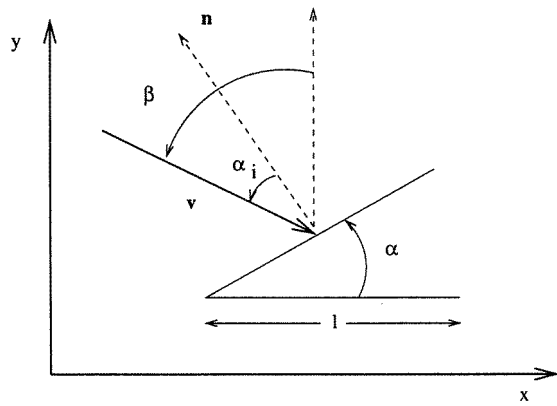


Figure 4. This figure defines angles α , α_i and β .

We now define α_i to be the angle made between the normal of the facets and the velocity vector at impact. Thus,

$$\alpha_i = \beta - \alpha. \tag{11}$$

In figure 7 we plot the distribution of α_i as determined from several values of the parameters ϵ and H . Surprisingly, we find that the different distributions collapse well to a single curve: the dependence on ϵ and H seems very weak, if indeed there is any. We see at present no

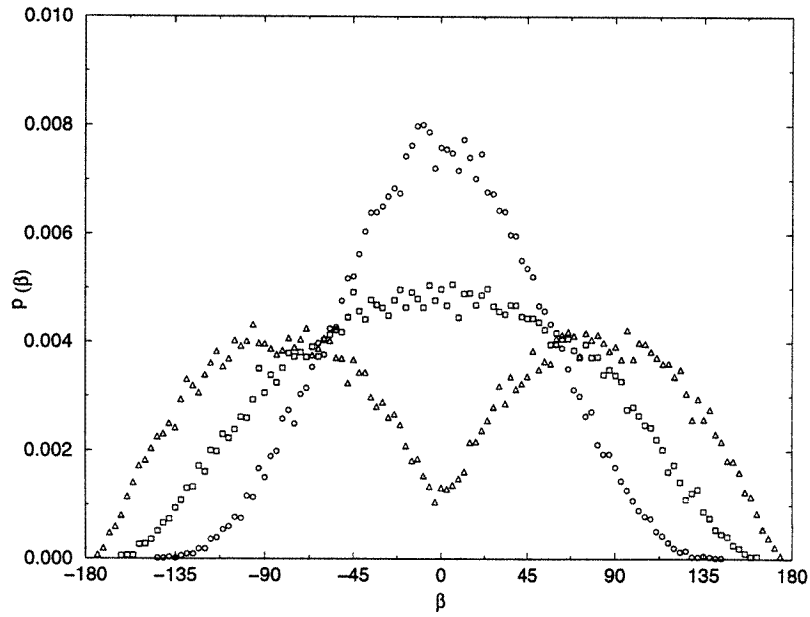


Figure 5. Distribution $p(\beta)$ for $H = 0.5$ different ϵ : circles correspond to $\epsilon = 0.547$, squares correspond to $\epsilon = 1.66$, and triangles correspond to $\epsilon = 11$.

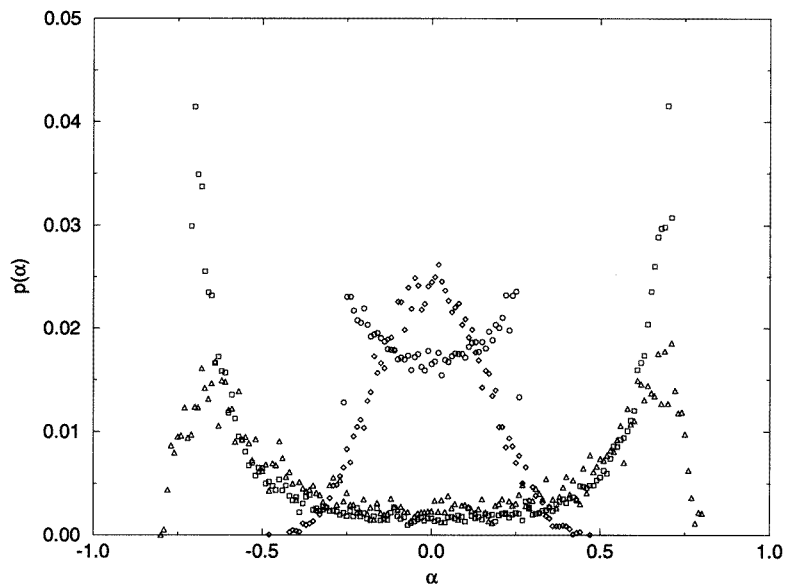


Figure 6. Distribution of tangents of the facets that were hit by the ball: circles correspond to $\epsilon = 0.274$ and $H = 0.5$, diamonds correspond to $\epsilon = 0.274$ and $H = 0.7$, squares correspond to $\epsilon = 1.6$ and $H = 0.5$, and triangles to $\epsilon = 1.6$ and $H = 0.7$.

convincing argument that explains this independence.

We now study the distribution of distances covered by the ball between impacts. We

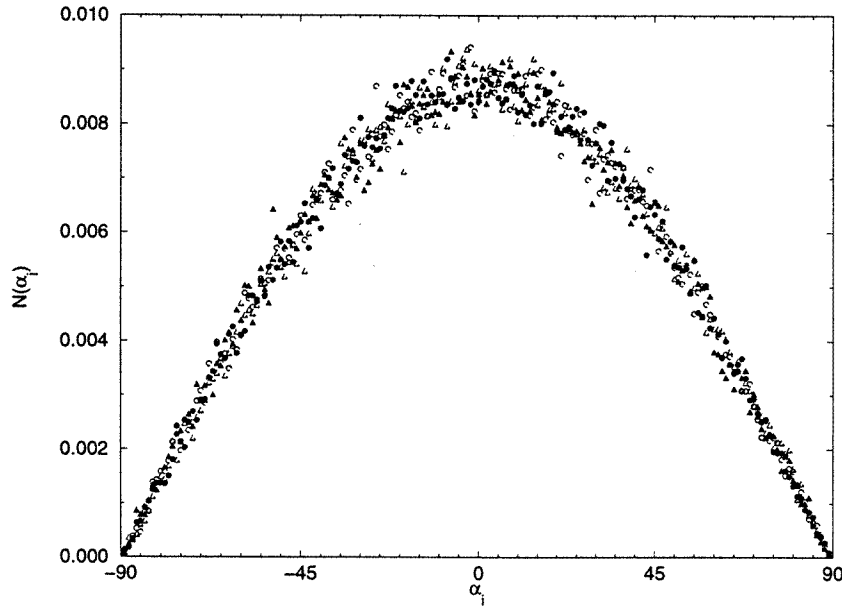


Figure 7. Distribution of α_i obtained for different ϵ and H : full circles correspond to $\epsilon = 2.19$ and $H = 0.5$, open circles correspond to $\epsilon = 2.19$ and $H = 0.7$, triangles pointing upwards correspond to $\epsilon = 0.274$ and $H = 0.5$, and triangles pointing downwards correspond to $\epsilon = 0.274$ and $H = 0.7$.

note the correspondence between this problem and that of a random walker in one dimension in the vicinity of an absorbing moving wall. When $H = \frac{1}{2}$, the profile may be seen as a one-dimensional random walker along the y -direction, while the x -direction corresponds to the time axis. The parabolic trajectory $Y(x)$ of the ball,

$$Y(x) = Y_0 + \frac{v_{y0}}{v_{x0}}(x - x_0) - \frac{g}{2} \left(\frac{x - x_0}{v_{x0}} \right)^2 \tag{12}$$

then corresponds to a moving wall, and we are asking the question when the two curves (profile and trajectory) cross for the first time. In (12), (x_0, y_0) and (v_{x0}, v_{y0}) are the coordinates and velocities at last impact. No analytic solution to this problem exists. However, if the ball were moving along a straight trajectory, $Y(x) = Y(x_0) + c(x - x_0)$, which is a good approximation as long as

$$x - x_0 \ll \frac{2}{g} v_{x0} v_{y0} \tag{13}$$

and

$$\frac{v_{y0}}{v_{x0}} = \mathcal{O}(\epsilon) \tag{14}$$

the distribution is of the jump size†

$$n(x_0, x) \propto \frac{e^{-c^2(x-x_0)/2\epsilon}}{(4\pi\epsilon(x-x_0))^{3/2}} \quad (16)$$

where $c = v_{y0}/v_{x0}$. For $c^2(x-x_0) \ll 2\epsilon$, $n(x_0, x) \sim (x-x_0)^{-3/2}$, which generalizes to

$$n(x_0, x) \sim (x-x_0)^{-(2-H)} \quad (17)$$

for general H in the same limit by the same arguments that led to equations (2) and (3) being a generalization of (7).

Equation (16) is a good approximation as long as there is a large horizontal velocity component and a small enough vertical velocity component so that there the ball hits the profile again before the parabolic component of its trajectory is becoming significant. Let us now assume the opposite limit, namely that v_{x0} is small and v_{y0} is large so that the parabolic component in (12) dominates, and that the amplitude of the roughness of the profile is small compared with the maximum height the ball reaches above the profile. In this case, the distribution $n(x_0, x)$ is well approximated by a Gaussian in $(x-x_0)$ with a well-defined average and variance. We demonstrate this in figure 8, where we use the parameters $A = g/2v_{x0}^2$ and $B = v_{y0}/v_{x0}$. The initial power-law behaviour with slope $2-H$ is clearly visible, as is the Gaussian-like hump for large intervals.

Figure 8 also demonstrates the scaling properties of the trajectory of the ball, equation (12), *vis-a-vis* the self-affine surface $y(x)$, which essentially behaves as $y(x) = \epsilon x^H$. Thus, by rescaling

$$\begin{cases} x \rightarrow \lambda x \\ \epsilon \rightarrow \eta \epsilon \end{cases} \quad (18)$$

we have

$$y \rightarrow \eta \lambda^H y. \quad (19)$$

If we now demand that the particle trajectory $Y(x)$ is to scale in the same way as y ,

$$Y \rightarrow \eta \lambda^H Y \quad (20)$$

we must rescale the parameters of the trajectory as follows

$$\begin{cases} g \rightarrow \eta \lambda^H g \\ v_{x0} \rightarrow \lambda v_{x0} \\ v_{y0} \rightarrow \eta \lambda^H v_{y0}. \end{cases} \quad (21)$$

Thus, parameters A and B defined above scale as $A \rightarrow \eta \lambda^{H-2} A$ and $B \rightarrow \eta \lambda^{H-1} B$. We may interpret this scaling as follows. Given two trajectories $Y_1(x)$ and $Y_2(x)$ characterized

† The probability density that a random walk starting at $y = 0$ and $x = 0$, for the first time hits the absorbing boundary $Y(x) = Y_0 + cx$ is

$$n(0, x) = \frac{Y_0 e^{-Y(x)^2/2x}}{(4\pi x)^{3/2}} \quad (15)$$

see, for example, [28]. In our case, $z(0) = 0$. However, our profiles are not continuous random walks, but consist of facets of finite size. Thus, the factor that should replace $Y(0) \rightarrow 0$ in our case is of the order of the size of the facets.

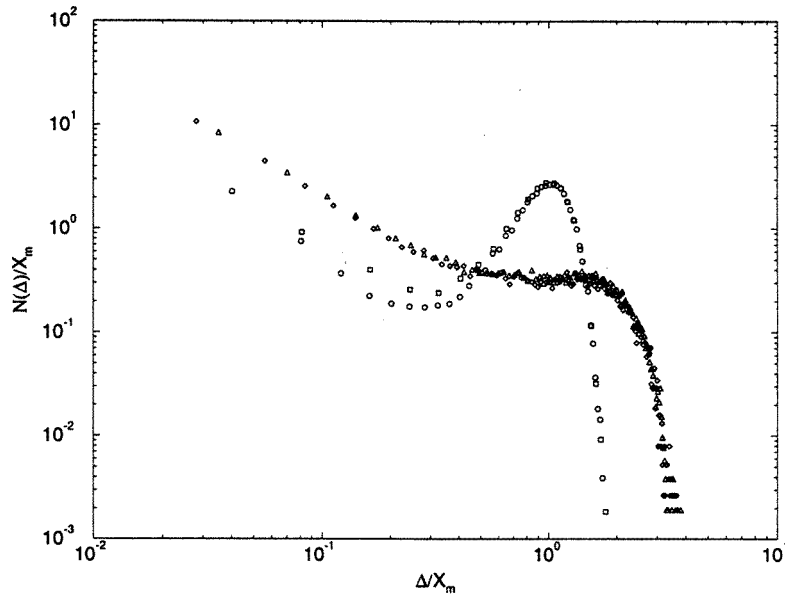


Figure 8. Distribution $n(x_0, x)$ of distance $(x_0 - x)$ between two consecutive contacts along a series of self-affine profiles with $H = 0.7$. There are four sets of data: (1) $A_1 = 0.01$, $B_1 = 0.5$, $\epsilon_1 = 0.4$, (2) $A_2 = 0.0742$, $B_2 = 1.83$ and $\epsilon_2 = 0.12$, (3) $A_3 = 0.07$, $B_3 = 5$ and $\epsilon_3 = 20$, and (4) $A_4 = 0.0939$, $B_4 = 5.35$ and $\epsilon_4 = 20$. Sets 1 and 2 are related through equation (21) with $\eta = 3$ and $\lambda = 0.5$, and sets 3 and 4 are related through equation (21) with $\eta = 1$ and $\lambda = 0.8$. The data sets have been shifted along both the horizontal and the vertical axes by a factor of X_m to demonstrate that there is data collapse between sets 1 and 2, and 3 and 4, but not between any other combination of data sets.

by parameters A_1 and B_1 and A_2 and B_2 , complete data collapse is possible between quantities measured from Y_1 and Y_2 if there exist an η and λ such that

$$\begin{cases} \frac{A_2}{A_1} = \eta\lambda^{H-2} \\ \frac{B_2}{B_1} = \eta\lambda^{H-1}. \end{cases} \quad (22)$$

This is demonstrated in figure 8, where we show the histogram of the jump lengths for trajectories based on four sets of parameters A_1 and B_1 to A_4 and B_4 . Pairs 1 and 2, and pairs 3 and 4 are related as in (22). We find data collapse between pairs 1 and 2, and 3 and 4, but not between any other combination.

We have presented a molecular dynamics study of the subsequent dissipation-free motion of a ball dropped onto a self-affine profile. The distribution of sizes of the energetically accessible intervals to which the ball is confined as a function of the height h at which the ball is dropped was determined. The average size of the intervals diverged. We studied the correlations between the distribution of slopes of the profiles and the distribution of directions of the velocity vector at impact, finding that the distribution of angles the velocity vector makes with the normal of the profile is independent of both H and the roughness amplitude. We studied the distribution of horizontal lengths of the parabolic trajectories of the ball between impacts. We found it to be a power law with exponent $H - 2$ for small lengths and Gaussian-like for large lengths. Finally, we have discussed how to scale the

parameters of the trajectories of the ball when rescaling the self-affine surfaces. We found that if the pairs of parameters could be related as in equation (22), the system, bouncing ball on a self-affine surface, is statistically invariant.

We have considered here only the simplest case: one-dimensional motion without dissipation. We are considering generalizations of this work along both of these axes, dissipation and two-dimensional motion.

Acknowledgments

We thank the CNRS and the NFR for support though the Franco–Norwegian *PICS* programme, and P C Hemmer for discussions.

References

- [1] Bideau D and Hansen A (ed) 1993 *Disorder and Granular Media* (Amsterdam: North-Holland)
- [2] Metha A (ed) 1994 *Granular Matter: An Interdisciplinary Approach* (Heidelberg: Springer)
- [3] Jaeger H M, Nagel S R and Behringer R P 1996 *Rev. Mod. Phys.* **68** 1259
- [4] Riguidel F X, Hansen A and Bideau D 1994 *Europhys. Lett.* **28** 13
- [5] Batrouni G G, Dippel S and Samson L 1996 *Phys. Rev. E* **53** 6496
- [6] Tufillaro N B and Albano A M 1986 *Am. J. Phys.* **54** 939
- [7] Everson R M 1986 *Physica* **19D** 355
- [8] Tufillaro N B, Mello T M, Choi Y M and Albano A M 1986 *J. Physique* **47** 1477
- [9] Mello T M and Tufillaro N B 1987 *Am. J. Phys.* **55** 316
- [10] Wiesenfeld K and Tufillaro N B 1987 *Physica* **26D** 321
- [11] Pierański P 1988 *Phys. Rev. A* **37** 1782
- [12] Metha A and Luck J M 1990 *Phys. Rev. Lett.* **65** 393
- [13] Franaszek M and Isomäki H M 1991 *Phys. Rev. A* **47** 4231
- [14] Boissel P 1992 *Bull. Union Physiciens* **86** 217
- [15] Luck J M and Metha A 1993 *Phys. Rev. E* **48** 3988
- [16] Devillard P 1994 *J. Physique I* **4** 1003
- [17] Schmittbuhl J, Vilotte J P and Roux S 1994 *J. Physique II* **4** 225
- [18] Hansen A, Engøy T and Måløy K J 1994 *Fractals* **2** 527
- [19] Chandrasekhar S 1943 *Rev. Mod. Phys.* **15** 1
- [20] Mandelbrot B B and van Ness J W 1968 *SIAM Rev.* **10** 422
- [21] Feder J 1988 *Fractals* (New York: Plenum)
- [22] Anderson P W 1978 *Les Prix Nobel 1977* (Stockholm: Almqvist and Wiksell)
- [23] Hansen A, Hinrichsen E L and Roux S 1991 *Phys. Rev. Lett.* **66** 2476
- [24] Poirier C, Ammi M, Bideau D and Trodec J P 1992 *Phys. Rev. Lett.* **68** 216
- [25] Horvath V, Kertesz J and Weber F 1993 *Fractals* **1** 67
- [26] Engøy T, Måløy K J, Hansen A and Roux S 1994 *Phys. Rev. Lett.* **73** 834
- [27] Cox D R and Miller H D 1965 *The Theory of Stochastic Processes* (London: Chapman and Hall)